Flavones enrich rhizosphere Pseudomonas to enhance nitrogen utilization and lateral root growth in Populus

Jianbo Xie

jbxie@bjfu.edu.cn

Beijing Advanced Innovation Center for Tree Breeding by Molecular Design, Beijing Forestry University, Beijing 10083

Deqiang Zhang

Beijing Forestry University

Jiadong Wu

Beijing Forestry University

Sijia Liu

Beijing Advanced Innovation Center for Tree Breeding by Molecular Design, Beijing Forestry University

Yue Wang

Beijing Advanced Innovation Center for Tree Breeding by Molecular Design, Beijing Forestry University

Jingna Si

Beijing Advanced Innovation Center for Tree Breeding by Molecular Design, Beijing Forestry University

Sisi Chen

Beijing Advanced Innovation Center for Tree Breeding by Molecular Design, Beijing Forestry University

Shuxian Tan

Beijing Advanced Innovation Center for Tree Breeding by Molecular Design, Beijing Forestry University

Yuxin Du

Beijing Advanced Innovation Center for Tree Breeding by Molecular Design, Beijing Forestry University

Zhelun Jin

Beijing Advanced Innovation Center for Tree Breeding by Molecular Design, Beijing Forestry University

Article

Keywords:

Posted Date: March 22nd, 2024

DOI: https://doi.org/10.21203/rs.3.rs-4090444/v1

Additional Declarations: There is **NO** Competing Interest.

Flavones enrich rhizosphere *Pseudomonas* to enhance nitrogen utilization and lateral root growth in *Populus*

Jiadong Wu[1,2,3,4†], Sijia Liu[1,2,3,4†], Yue Wang[1,2,3,4†], Jingna Si[1,2,3,4], Sisi Chen[1,2,3,4], Shuxian Tan[1,2,3,4], Yuxin Du[1,2,3,4], Zhelun Jin[1,2,3,4], Jianbo Xie[1,2,3,4*] and Deqiang Zhang[1,2,3,4*]

[†]Jiadong Wu, Sijia Liu and Yue Wang contributed equally to this study

[1]State Key Laboratory of Tree Genetics and Breeding, College of Biological Sciences and Technology, Beijing Forestry University, Beijing 100083, China;

[2]National Engineering Research Center of Tree Breeding and Ecological Restoration, College of Biological Sciences and Technology, Beijing Forestry University, No. 35, Qinghua East Road, Beijing 100083, P. R. China;

[3]Key Laboratory of Genetics and Breeding in Forest Trees and Ornamental Plants, Ministry of Education, College of Biological Sciences and Technology, Beijing Forestry University, No. 35, Qinghua East Road, Beijing 100083, P. R. China;

[4]The Tree and Ornamental Plant Breeding and Biotechnology Laboratory of National Forestry and Grassland Administration, Beijing Forestry University, No. 35, Qinghua East Road, Beijing 100083, P. R. China;

[5]State Key Laboratory of Subtropical Silviculture, Zhejiang A&F University, Hangzhou, Lin'an, China

E-mail addresses: Jiadong Wu – jiadongwu@bjfu.edu.cn; Jianbo Xie – jbxie@bjfu.edu.cn; Deqiang Zhang – DeqiangZhang@bjfu.edu.cn.

*To whom correspondence should be addressed. Tel: +86-10-62336007; Fax: +86-10-62336164. E-mail: jbxie@bjfu.edu.cn and DeqiangZhang@bjfu.edu.cn

Abstract

Plant growth behavior is a function of genetic network architecture. The importance of root microbiome variation driving plant functional traits is increasingly recognized, but the genetic mechanisms governing this variation are less studied. Here, we collected roots and rhizosphere soils from nine *Populus* species belonging to four sections, generated metabolite and transcription data for roots and microbiota data for rhizospheres, and conducted comprehensive multi-omics analyses. We demonstrated that the roots of robust *Leuce* poplar enriched more plant growth-promoting rhizobacteria, which compared with the poorly performing poplar, agreeing with the 'Matthew effect' on poplar-microbe interaction. Moreover, we confirmed that *Pseudomonas* was strongly associated with tricin and apigenin biosynthesis and identified that gene *GL3* was critical for tricin secretion. The elevated tricin secretion via constitutive transcription of *PopGL3* and *PopCHS4* could drive *Pseudomonas* colonization in the rhizosphere and further enhance poplar growth, nitrogen acquisition, and lateral root development in nitrogen-poor soil. This study reveals plant-metabolite-microbe regulation patterns contribute to the poplar fitness and thoroughly decoded the key regulatory mechanisms of tricin, and provided new insights into the interactions of the plant's key metabolites with its transcriptome, rhizosphere microbes.

Introduction

Rhizosphere microbial community structure is highly dynamic in part due to the changes in root exudation over the course of plant development[1-4]. Although some chemical signals released by plants facilitate specific interactions, many have been recognized by previous studies. For example, flavonoids (luteolin, apigenin, etc.) could interact with rhizobial *NodD* proteins activating the transcription of nodulation genes responsible for the deformation of plant root hairs and assisting rhizobial entry via infection threads[5,6]; coumarins induce the colonization of *Pseudomonas simiae* ACS417 and promote the growth and health of the host plant[7]. Further, studies in oat (*Avena strigosa*) found that mutants lacking avenacins have different culturable communities of root-colonizing fungi[8] and are more susceptible to fungal pathogens than isogenic wild-type oat[9]. Surprisingly, however, a recent global analysis of the rhizosphere microbiome of these two oat genotypes found strong differences between eukaryotic Amoebozoa and Alveolata, whereas bacterial communities were unaffected[10]. This highlights that variation in plant genotype can have complex and unforeseen effects on the plant microbiome.

Poplar (*Populus* L.), a globally cultivated fast-growing and high-yielding timber tree species, comprises five sections: *Leuce*, *Aigeiros*, *Tacamahaca*, *Turanga*, and *Leucoides*[11]. Distinct poplar genotypes exhibit various growth characteristics[12,13], and these differences profoundly influence the productivity and adaptability of the poplars[14,15], because the enhancement of certain growth traits may be closely linked to a plant's resistance to environmental stressors[16,17]. The fast-growing *P.* × *euramericana* Dode manifests a more developed root system than the slow-growing *P. simonii* Carr, concurrently displaying heightened capabilities for phosphorus/nitrogen uptake and assimilation, promoting growth in phosphorus and/or nitrogen-deficient environments[14]. Additionally, diverse poplar genotypes (or sexes) shape rhizosphere communities by recruiting specific microbial taxa[18-20], under which microbes may alter host performance and fitness directly or via ecosystem services such as nutrient

accessibility[21-23]. However, the mechanism by which poplar genotypes regulate microbial communities overall assembly and functional changes remains largely unclear, as are the effects of host genotype-selected rhizosphere microbiomes on poplar growth and fitness.

Recent studies have uncovered several plant key genes involved in the structuring of rhizosphere microbial communities[24-26]. Evidently, this is essentially a 'top-down' regulatory process, in which functional genes alter rhizosphere microbial community composition based on the regulation of metabolites or other signaling molecules[3,7,25]. Previous studies have effectively integrated plant transcriptomics with microbiome community data using methods such as Weighted Gene Co-Expression Network Analysis (WGCNA)[27] and Microbiome-Wide Association Studies (MWAS) analyses[28,29], demonstrating that host gene expression indeed influences the composition of the microbial community. However, analyzing the correlation between the gene-microbe factors cannot truly elucidate the regulating pathways from a multi-omics perspective. The establishment of a comprehensive network involving genes, metabolites, and rhizosphere microbes becomes crucial for a thorough understanding of plant-microorganism interactions.

In the study, the transcriptome, metabolome, and microbiome datasets across various poplar genotypes were combined to establish a comprehensive gene-metabolite-microbe network. By using this multidimensional dataset, the regulating chains that how poplar recruiting target beneficial microbes and how the microbes affect the host's fitness were constructed. The function of the key genes was further investigated by using molecular analyses. We highlight how root exudates, the rhizobiome, and their mutual interactions affect host fitness and how these explicitly processes occurred in our investigations of belowground plant-rhizobiome interactions.

Results

Robust species become more robust by shaping the root microbial community

To assess the importance of the root microbiome in plant fitness, we performed a pot experiment on poplar grown in a natural soil mixture (low nitrogen; total nitrogen: 0.089%). After three months of growth, eleven phenotypes of the nine representative poplar species derived from four sections (*Leuce*, *Aigeiros*, *Tacamahaca,* and *Turanga*) were examined (Supplementary Fig. 1). Results indicated that seedlings from *Leuce* demonstrated the most superior biomass, followed by *Aigeiros* and *Tacamahaca*, while *Turanga* exhibited the lowest (ANOVA, *P*-values < 0.01; Supplementary Fig. 1C, D). The growth parameters varied among species. For example, mean root biomass ranged from 0.56 to 15.76 g, plant height ranged from 27.02 to 129.91 cm, and leaf area ranged from 1.06–76.30 cm^2. Notably, the shoot biomass of the fast-growing *P. tomentosa* Lumao 50 (LM50) was 14.02 times greater than the slowest-growing *P. euphratica* H (Peu-H). These findings indicate substantial variations in growth performance among distinct sections of poplar under controlled conditions.

To investigate whether genotype-mediated soil microbiota was involved in shaping disparities in poplar growth, a follow-up soil transplant experiment was conducted on the vigorous LM50 and the poorly performing Peu-H. When Peu-H was transplanted into soil in which LM50 had previously been grown (LM50-grown soil), Peu-H significantly increased shoot biomass compared with soil in which Peu-H had previously been grown (Peu-H-grown soil; an increase of 27.22%; ANOVA, *P*-values < 0.01; Fig. 1A, B). In contrast, LM50 showed significant growth inhibition when transplanted into Peu-H-grown soil compared with LM50-grown soil (a reduction of 19.58%; ANOVA, *P*-values < 0.01; Fig. 1A, B). It is noticeable that LM50 produced 7.37 g more shoot biomass than Peu-H in sterilized soil, nevertheless this discrepancy widened to 8.29 g (Peu-H-grown soil) and 10.26 g (LM50-grown soil), respectively (Fig. 1A, B). A similar trend was also observed in *P. alba* × *P. glandulosa* 84K (84K; *P*-values < 0.05; Supplementary Fig. 2A–C). Notably, root exudates from all genotypes

had no significant effect on poplar biomass in sterilized soil (Supplementary Fig. 2D–F). These results demonstrate that plant-associated microbiota positively influences poplar growth, but the extent of this effect varies depending on plant genotype. Specifically, the root microbial community shaped by the vigorous genotype was more conducive to plant growth, whereas the promoting effect of the root microbial community recruited by the less robust genotype was weaker.

Taxonomic features of the rhizosphere microbial composition between poplar

To evaluate the impact of the different poplar genotypes on the rhizosphere microbiome composition and functional potential, samples of bulk soil and rhizosphere soil were collected. Bacterial community composition across the nine poplar species was investigated for each sample type (bulk soil and rhizosphere soil) using Illumina MiSeq sequencing of the V3–V4 region of the 16S rRNA gene. Across sections, *Turanga* showed the highest diversity in rhizosphere microbiota, followed by *Aigeiros*, *Tacamahaca*, and *Leuce* (ANOVA, *P*-values < 0.05; Supplementary Fig. 3A). By contrast, there was no significant difference among bulk soil samples. It is evident that plant genotype affects the process of rhizosphere microbial recruitment.

The compositional volatility of the rhizosphere microbiome among the four sections is driven by significant shifts in the relative abundance of nineteen specific bacterial phyla (LDA score > 2, Kruskal-Wallis test, FDR adjusted *P*-values < 0.05; Fig. 1C, Supplementary Fig. 3B, and Supplementary Data 3). At the genera level, we identified 82 specific markers in *Turanga,* compared to those exclusively found in *Aigeiros* (28 genera), *Tacamahaca* (23 genera), and *Leuce* (11 genera; LDA score > 2, Kruskal-Wallis test, FDR adjusted *P*-values < 0.05; Fig. 1C). We noticed that several plant growth-promoting rhizobacterias (PGPRs) such as Actinobacteriota and *Tumebacillus* were highly abundant in the *Turanga*. These microbes have been reported to be associated with plant growth and stress responses[3,30,31]. The PGPR *Bacillus*, known for promoting plant growth through the production of hormone and nitrogen fixation, was found to be enriched in *Aigeiros*[32]. Notably, the eleven marker genera

detected in *Leuce* accounted for 26.43%–54.05% of the relative abundance, including *Pseudomonas* (7.93%–26.42%) and *Cellvibrio* (9.70%–17.82%). The PGPRs *Pseudomonas*, *Pseudoxanthomonas*, and *Cellvibrio* have been demonstrated to enhance plant growth through the processes of biological nitrogen fixation or polycyclic aromatic hydrocarbon degradation[33-35]. Therefore, the specific recruitment of these high-abundance beneficial bacteria by *Leuce* may have been the reason why its root microbial community was more conducive to plant growth. Together, these results indicate that genotype properties establish root-inhabiting bacterial communities by selecting specific microbial taxa that are associated with plant nutrition and growth performance.

Co-expression network of gene expression, flavonoid productions, and rhizosphere microbial community

To guide our efforts to investigate molecular mechanisms during rhizosphere microbial recruitment in poplar, we generated 73.7 Gb of root transcriptomic data across nine poplar species. This identified 38,739 expressed genes (TPM > 0). The Principal Component Analysis (PCA) and Hierarchical Clustering Analysis (HCA) based on all microbial (OTU > 2; Fig. 1D, G), phenotypic (Fig. 1E, H), and transcriptomic (Fig. 1F, I) data clearly classified the nine poplar species into four distinct subgroups. This indicates a strong impact of poplar genetic regulation on the composition of the rhizosphere microbiome. Functional enrichment analyses revealed that differentially expressed genes (DEGs; $|\log2FC| > 1$, *P*-values < 0.05; Supplementary Fig. 4 and Supplementary Data 4) were overrepresented in functions related to flavonoid metabolism (*P*-values < 0.05; Supplementary Fig. 5 and Supplementary Data 5). Flavonoids play vital roles in the assembly of plant root microbiome communities, such as the roots of Arabidopsis (*Arabidopsis thaliana* L.) and maize (*Zea mays* L.)[36,37]. This suggests that flavonoid metabolism may vary in poplar roots and mediate the composition of the rhizosphere microbial community.

Next, we quantified 129 flavonoids from the root samples of nine poplar species, of which 110 (85.27%) were differentially accumulated in at least two species (|log2FC| > 1.585, *P*-values < 0.05; Supplementary Data 6). To gain further insights into the gene-metabolites-microbiome regulatory network, the 110 differential flavonoids, 17,997 DEGs, and 397 OTUs were further classified into six co-expression clusters using the *k*-means clustering algorithm and Pearson's correlation analysis ($r \geq 0.7$, *P*-values < 0.01; Fig. 2, Supplementary Fig. 6, and Supplementary Data 7). These clusters demonstrated a unified and distinct abundance pattern related to specific sections, such as *Turanga* (Cluster I), *Leuce* (Cluster IV), and *Aigeiros* (Cluster V). Interestingly, after removing genes and OTUs that were not highly correlated with any of the flavonoids, the PCA (Supplementary Fig. 7A, B) and HCA (Supplementary Fig. 7C, D) analyses still showed clustering patterns similar to the subgroups of global genes and microbes. All together, these results indicate that the trends of gene expression, flavonoid accumulation, and rhizosphere microbial enrichment show significant section specificity.

We identified 159 candidate genes encoding enzymes that catalyze the twelve enzymatic reaction steps of the flavonoid biosynthesis pathway (Supplementary Data 7). Four out of thirteen *CHS* genes and all three *F3'H* genes were present in Cluster IV, where *F3'H* plays a pivotal role in catalyzing the conversion of naringenin to eriodictyol and dihydrokaempferol to dihydroquercetin, crucial precursors in the biosynthesis of flavones and flavanols[38,39]. Correspondingly, eleven (11/21) flavones were observed in Cluster IV. Among them, apigenin (methylApigenin C-pentoside) could recruit beneficial bacteria such as *Rhizobium*, Oxalobacteraceae, and *Pseudomonas*, enhancing the plant's nitrogen uptake capacity[36,40,41]. Notably, our findings revealed the presence of 28 bHLH and 39 MYB transcription factors in Cluster IV. Members of the two gene families often synergistically regulate flavonoid biosynthesis[42,43]. Moreover, two *FLS* genes and seven (7/16) flavonols were highly correlated in Cluster V. Therefore, the co-expression network facilitates elucidating the genetic mechanisms of microbial recruitment and identifying candidate genes.

Gene expression and flavonoid accumulation were consistent with rhizosphere microbial composition and poplar growth performance

To further enrich putative regulating networks, we specifically focused on Cluster IV and Cluster I, which were abundant in the *Leuce* and *Turanga*, respectively (Supplementary Fig. 6A–C), as the two sections demonstrated the most contrasting growth performances (Supplementary Fig. 1C, D). Functional enrichment analyses showed genes in Cluster I (enriched in *Turanga*; |log2FC| > 1, *P*-values < 0.05; Supplementary Data 4) were mainly associated with housekeeping functions such as genetic information processing, ribosome biogenesis, and mismatch repair (*P*-values < 0.05; Supplementary Fig. 8A; Supplementary Data 5). By contrast, genes in Cluster IV (enriched in *Leuce*; |log2FC| > 1, *P*-values < 0.05; Supplementary Data 4) are involved in energy and matter cycles (carbon fixation in photosynthetic organisms, starch and sucrose metabolism, nitrogen metabolism, and energy metabolism), as well as flavonoid metabolism (phenylalanine metabolism, phenylpropanoid biosynthesis, and flavonoid biosynthesis; *P*-values < 0.05; Supplementary Fig. 8B; Supplementary Data 5).

We found that OTUs in Cluster I and Cluster IV were associated with nutrient cycles, particularly nitrogen metabolism and transformation (Supplementary Fig. 9A; Supplementary Data 8). In Cluster I, OTUs showed enrichment in functions of nitrate reduction and nitrogen respiration, contributing to denitrification and accelerating nitrogen depletion in the soil (enriched in *Turanga*; ANOVA, *P*-values < 0.01; Supplementary Fig. 9D, E)[44]. Conversely, OTUs of Cluster IV exhibited enrichment in functions related to nitrogen fixation and cellulolysis (enriched in *Leuce*; ANOVA, *P*-values < 0.01; Supplementary Fig. 9B, C). We then look into how metabolite accumulation influences microbes. The flovnes, tricin and apigenin (with their derivatives), were uncovered in Cluster IV, which were the most enriched metabolites in *Leuce* (ANOVA, *P*-values < 0.01; Fig. 3A). Tricin is structurally similar to apigenin and shares the same KEGG pathway as apigenin (ko00944), suggesting that tricin may have a similar biological function to apigenin (Fig. 3B). Based on these results, we

hypothesized that the secretion of flavones of *Leuce* roots may recruit specific beneficial bacteria to promote plant nutrient absorption and growth.

In order to investigate how gene expression and flavonoids influenced the abundance of the microbial community and growth performance, we performed detailed analyses of the subnetwork of gene, flavone, microbe, and trait modules (*P*-values < 0.01; Fig. 3C). Consistent with our expectations, the expression of genes in the flavonoid metabolism (phenylalanine metabolism, phenylpropanoid biosynthesis, and flavonoid biosynthesis) showed a significant positive correlation with the accumulation of apigenin and tricin. The accumulation of apigenin and tricin was associated with microbe modules with functions of nitrogen metabolism (nitrogen fixation, nitrate reduction, and nitrogen respiration). Notably, Pseudomonadaceae, Cellvibrionaceae, and Alicyclobacillaceae were among the top families showing the highest correlation with flavone modules and flavonoid-related gene modules (*P*-values < 0.01; Fig. 3D). Pseudomonadaceae, one of the most abundant taxa in the poplar rhizosphere, was specifically enriched in *Leuce* and correlated with poplar growth (ANOVA, *P*-values < 0.01; Fig. 3E, F and Supplementary Fig. 9F). In particular, at the genus level, *Pseudomonas,* which has been demonstrated as a PGPR with beneficial potentials in nitrogen fixation, phosphorus solubilization, secretion of growth hormones, and antimicrobial activities[33,45], was strongly correlated with plant growth characteristics (*P*-values < 0.01; Fig. 3G and Supplementary Fig. 9G). Overall, these results showed that flavonoid pathway genes in *Leuce* roots regulate the secretion of flavones to enrich specific beneficial bacteria, thereby promoting poplar nitrogen metabolism and growth.

Tricin and apigenin mediated pseudomonads enhancing nitrogen utilization and secondary root growth in poplar

We further isolated eleven *Pseudomonas* strains from rhizosphere soil samples of *Leuce*, and the 16S rRNA genes of nine isolates exhibited highly homologous (> 98%) to OTUs of Cluster IV (Supplementary Data 9). Further characterization showed that seven

isolates possessed the capacity for nitrogen fixation and carried the *nifH* gene, and eight isolates demonstrated the secretion of indole-3-acetic acid (IAA; Supplementary Fig. 10A–D). Notably, Pto1, Pto5, and Pto10 enhanced swarming motility in the presence of 5 μM tricin and 100 μM apigenin (Fig. 4A). qRT-PCR analysis suggests that flagellar-related genes (*motA, fliG,* and *bifA*) [40] and biofilm formation-related gene *algU* were activated[46], which may critical for successful bacterial root colonization (*P*-values < 0.01; Fig. 4B).

To investigate the potential of *Pseudomonas* isolates on poplar fitness, we inoculated three individual strains and constructed synthetic communities (SynComs: Pto1, Pto5, and Pto10). Using ^{15}N isotope labeling, we traced the nitrogen absorbed by poplar from soil, while nitrogen fixed by microbes from the air remained unlabeled. Inoculated isolates significantly increased the shoot biomass (26.04%–48.03%), root biomass (57.51%–81.46%), and leaf nitrogen content (7.98%–10.15%) of poplar (ANOVA, *P*-values < 0.01; Fig. 4C, D and Supplementary Fig. 11A). Similar trends were also observed in other plant species (*P*-values < 0.01; Supplementary Fig. 12). After inoculation, the ^{15}N ratio of leaves of inoculated isolates decreased, indicating that pseudomonads promoted the nitrogen absorption of poplar through biological nitrogen fixation (BNF; SupplementalryTable 1). Consistently, in sterile nitrogen-poor medium, the number and length of poplar secondary roots (SRs) increased by 9.92 and 2.88 times after inoculation with Pto1, respectively (*P*-values < 0.01; Fig. 4E, F). However, the promoting effects of Pto1 on poplar growth and SR induction were diminished in a medium with sufficient nitrogen supply (Fig. 4F and Supplementary Fig. 11B). These results suggest that the functions of pseudomonads may rely on the cross-talk between specific nitrogen starvation signaling and plant responses.

Pto1 induces the *PLT3PLT5PLT7*-mediated LR pathway by secreting IAA

The intricate architecture of the root system in Arabidopsis has multiple types of SRs, encompassing lateral roots (LRs), adventitious lateral roots (adLRs), and adventitious roots (ARs), which are regulated by distinct genetic pathways[47-50]. To elucidate the

nature of the induced SRs following inoculation with Pto1, we conducted a structural analysis of the root systems of the *plt3plt5plt7* triple mutant, which exhibits compromised LR formation, and the *wox11wox12* double mutant, displaying deficiencies in adLR and AR formation[51]. In the *plt3plt5plt7* mutants inoculated with Pto1, no visible SR was observed at 7 d (Fig. 4H, I). Conversely, the *wox11wox12* mutants exhibited a significant increase in the number of SRs, comparable to the increase observed in wild-type roots following Pto1 inoculation. When IAA was added to the medium, the development pattern of Arabidopsis roots was similar to that resulting from Pto1 inoculation. However, the auxin inhibitor 2,3,5-triiodobenzoic acid (TIBA) hindered SR growth in all Arabidopsis lines, regardless of the presence of Pto1. These results suggest that Pto1 inoculation induces the LR pathway mediated by *PLT3PLT5PLT7* through the secretion of IAA.

PopGL3 **regulated the synthesis of tricin to recruited** ***Pseudomonas***

We conducted an analysis of the co-expression network to identify novel regulators associated with flavone biosynthesis, given its significance in microbial recruitment. In Cluster IV, which enriched apigenin and tricin, a member of the bHLH transcription factor family, *bHLH1* (also known as *GL3*) was identified (enriched in *Leuce*; ANOVA, *P*-values < 0.01; Supplementary Fig. 13A). It exhibited strong co-expression with flavones and genes related to flavonoid biosynthesis (Supplementary Fig. 13A). *GL3* was reported to interact with MYB transcription factors and WD40 repeat proteins to form the MYB-bHLH-WD40 (MBW) transcriptional complex, regulating anthocyanin synthesis[52,53]. However, the potential roles of *GL3* in flavone synthesis and interactions with the rhizosphere microbiome remain unclear. DAP-seq experiment revealed that *PopGL3* could regulate the transcription of *PopPA2*, *PopF3'H*, *PopDAHP*, *PopCCR1*, and *PopTHB*, which are involved in flavonoid synthesis (Fig. 5A, B). Notably, *F3'H* catalyzes the conversion of flavone precursors into flavones (Fig. 5C). The constitutive expression of *PopGL3* could activate the transcription of *PopF3'H* and *PopFNS* and release more tricin in the rhizosphere of the *PopCHS4-OE* (chalcone synthase catalyzes

the first committed step of the multi-branched flavonoid pathway) and *PopGL3-OE* lines (*P*-values < 0.01; Fig. 5 E, F).

Following two months of growth in unsterilized nitrogen-poor soil (with a small amount of ^{15}N-labeled ammonium nitrate), *PopGL3-OE* and *PopCHS4-OE* plants displayed increased biomass and leaf nitrogen accumulation (*P*-values < 0.01; Fig. 5D, G and Supplementary Fig. 13B, C). Compared with the wild-type, the contribution of BNF by transgenic plant root microorganisms increased (Supplementary Table 2). Conversely, all genotypes grew weakly in sterilized soil, with no difference in biomass production. However, our amplicon sequencing results indicated that transgenic plants reshaped the rhizosphere microbial composition and significantly enriched *Pseudomonas* (*P*-values < 0.01; Fig. 5H, I and Supplementary Fig. 13D, E).

Evidence from our experiment suggests that the increased abundance of *Pseudomonas* in the transgenic plants is like due, in part, to the greater absolute depletion of most other bacterial lineages, but does not rule out the positive selection by the transgenic plants through the tricin pathway. To confirm the increased root colonization of *Pseudomonas* in the transgenic plants, we tagged Pto1 with RFP fluorescence gene and used confocal microscopy to image the colonization of root tissue across various genotypes. We observed significantly enhanced colonization and increased fluorescence density in the roots of *PopGL3-OE* and *PopCHS4-OE* plants using confocal microscopy (*P*-values < 0.01; Fig. 6A, B). In conclusion, *PopGL3*, a novel regulator of flavone biosynthesis, recruits *Pseudomonas* by secreting tricin to promote the growth and nitrogen uptake of poplar. Taken together, these data suggest that in a controlled laboratory setting and in the absence of other microbes, the observed increase in *Pseudomonas* abundance in the *PopGL3-OE plants* is accompanied by increased colonization, and that this increase is potentially beneficial to poplar fitness.

Discussion

Given the importance of the rhizomicrobiome in plant development, nutrition acquisition, and stress tolerance, deciphering the molecular regulatory network of plant-

microbe interactions could substantially contribute to improving plant yield and quality. Current multi-omics studies of plant-microbial interactions have mostly relied on methods such as WGCNA and MWAS, which are confined to the analysis of these binary transcriptome-microbiome datasets, often failing to effectively find metabolites (or other signaling molecules) that directly shape the structure of plant microbial communities[27-29]. In this study, a dataset comprising gene expression, metabolic profiling, and microbial community derived from four sections of poplar was generated, constructing a comprehensive gene-metabolic-microbe co-expression network. Within this network, we've unveiled the pivotal role of flavonoids in shaping the composition of the poplar root-associated microbial community, particularly in their intimate associations with beneficial microbes like *Pseudomonas*, *Bacillus*, and Actinobacteriota, known to confer advantages to plant fitness[3,51,54]. The investigation within the network not only unveils intricate linkages between plant genetic regulation and metabolite synthesis but also elucidates the direct influence of these metabolites on the structure of microbial communities, offering valuable guidance for future experimental designs.

In response to biotic or abiotic stresses, plants employ a 'cry for help' strategy, recruiting beneficial microorganisms to help them resist these stresses through the secretion of various chemical compounds[37,55-57]. Flavonoids, a major category of specialized metabolites in plants, significantly influence plant growth and development, and play a critical role in mediating several plant-microbe interactions[1,58]. For instance, maize FNSI2-mediated apigenin and luteolin have been shown to enhance the abundance of Oxalobacteraceae in the plant rhizosphere, improving host performance under nutrient-limiting conditions[36]. Consistent with these observations, the biomass of LM50 (*Leuce*) was greater than that of Peu-H (*Turanga*) in sterile and nitrogen-poor soil, while the biomass of both increased in unsterilized soil, but the difference between them expanded further, indicating that genotype-cried microbiota exerts varying degrees of positive feedback on poplar growth. Correlation analysis revealed that Leuce-enriched flavonoid gene modules and flavone modules exhibited the strongest association with Pseudomonadaceae, while the increased abundance of

Pseudomonadaceae and *Pseudomonas* was highly correlated with poplar's growth characteristics.

Experiments have shown that apigenin and tricin (in Cluster IV) enhance the swarming motility and biofilm synthesis of pseudomonad isolates, and this flavone-mediated mechanism significantly promotes the mobility of the pseudomonads at the soil/root interface, favoring the successful colonization of the plant root surface[40]. We identified the transcription factor *PopGL3* (in Cluster IV) that activates *PopF3'H* and *PopFNS* expression. Rhizosphere microbiome analyses of *PopGL3* and *PopCHS* transgenic plants, integrating the metabolite profiles of root extracts and secretions, demonstrate the causal role of *PopGL3* in tricin secretion and recruitment of *Pseudomonas*. A series of inoculation experiments with tricin-mediated isolates confirmed their beneficial effects on poplar growth, nitrogen accumulation, and LR growth. These findings suggest that the poplar *GL3* gene regulates tricin synthesis and secretion to call for pseudomonad colonization to help it grow and nitrogen absorption in nutrition-deficient conditions.

Previous studies believed that the core microbes determined the function of the plant microbiome[59-61]. However, there was almost no difference in the core microbial taxa of the same plant species under the same environment[62,63], and *Pseudomonas* had a certain advantage in the rhizosphere of all poplar sections. Therefore, differences in the host's ability to 'cry for help' to beneficial microorganisms lead to different degrees of feedback from recruited microorganisms on their own fitness. This disparity, possibly regulated by plant genes, signifies that robust *Leuce* elevated the tricin secretion via heightened *GL3* expression, driving pseudomonad colonization in the rhizosphere and enhancing growth, nitrogen acquisition, and lateral root development in nitrogen-poor soil (Fig. 7). Consistent with our finding, plant resistance genes *GsMYB10* transgenic soybean recruited *Bacillus* and *Aspergillus*, which in turn enhanced plant resistance to stresses under aluminum (Al) toxicity[64]. In this context, we introduce the concept of the 'Matthew effect' in plant-microbial interactions for the first time. That is, robust or resistant plant genotypes can recruit specific microbes to give them more growth advantages or better resistance. Parallelly, this effect is also

reflected in the interaction between microbes and roots. Root caps and root hairs serve as crucial determinants for the assembly process of the rhizosphere microbiome[65,66]. As the quantity and length of LR increase, the spatial distribution of plant-secreted nutrients and metabolites also expands, enhancing the plant's regulatory influence over the rhizosphere microbial community. Conversely, the rhizosphere's available area for microbial colonization expands with the development of LRs, prompting enhanced beneficial activities by microorganisms toward the plant. This is consistent with previous studies showing that the assembly process of plant rhizosphere microorganisms is closely related to plant root structure[67-69].

Although the clustering patterns of DEGs and OTUs strongly associated with flavonoids are consistent with global genes and microbes, some compounds, such as hormones and terpenoids, were not quantified in our samples due to the limited scope of detection in this study. Additionally, the root endosphere microbiome or fungi were not also tested. When we obtain this information, the number of genes and microbes co-expressed with metabolites is likely to increase further, providing a richer resource for in-depth investigations of the plant genetic networks that regulate the recruitment of microbes by metabolic pathways.

Materials and methods

All other methods used in this study are described in the Supporting Information (Supplementary Methods 1–14).

Plant and soil materials, growth conditions

Nine species of poplars from four sections, *Leuce* (*Populus tomentosa* × *P. bolleana* M 'Pto-M', *P. alba* × *P. glandulosa* 84K '84K', *P. alba* × *P. glandulosa* Y 'Pal-Y', *P. tomentosa* Lumao50 'LM50'), *Aigeiros* (*P. euramericana* 74/76 '107', *P. euramericana* H3-1 'H3-1'), *Tacamahaca* (*P. trichocarpa* M 'Pot-M', *P. szechuanica* Z 'Psz-Z'), and *Turanga* (*P. euphratica* H 'Peu-H'), were examined in this study. Tissue culture plantlets of poplar clones (84K, Pse-Z, Ptr-M, and Peu-H) were maintained in our

laboratory, while the remaining five species were collected from the GuanXian state-owned *P. tomentosa* forest farm in Shandong Province, China (E: 115°22'8", N: 36°30'54") to acquire sterile monoclonal tissue culture seedlings.

The soils of *Leuce*, *Aigeiros*, and *Tacamahaca* were collected from the plantations of *P. tomentosa*, *P. euramericana*, and *P. simonii* in the GuanXian state-owned forest farm, respectively, while the soil of *Turanga* was collected from the natural forest of *P. euphratica* in Danglang tribe, Aksu, Xinjiang (E: 80°15'18", N: 40°45'39"). Notably, these forests, aged over 15 years, have never received fertilization. Removed the surface 10 cm of soil, and at the surface 10–40 cm of soil around the poplars was collected, with each soil taken from at least five poplars.

Four parts of soil were mixed in equal volumes and thoroughly stirred. Subsequently, tissue culture seedlings of the nine poplar species were simultaneously transplanted into the mixed soil for pot experiments, ensuring at least five biological replications per species while randomly situating all poplar samples. They were grown in the same environment for three months, with fertilizer required for growth once at the beginning and water poured every two days.

Plant measurements and sample collection

On the day of destructive sampling, we examined eleven representative characteristics encompassing morphological and structural (growth traits: plant height, ground diameter, shoot biomass, root biomass, and root length; leaf traits: leaf length, leaf width, leaf area, and leaf number), physiological functional (chlorophyll content), and component content (leaf nitrogen content) aspects of nine poplar species. Three plants of comparable growth were selected as biological replicates, except for Peu-H, where two individual plants were pooled as one biological replicate. Leaf length and width of the third, fourth, and fifth completely expanded leaves at the top were measured, and the leaf area was calculated by ImageJ (v.1.53q)[70] analysis. Leaves were defined as fully expanded if the leaf length was more than 4.0 cm. Chlorophyll content was determined as the average of 20 measurements with a chlorophyll meter (SPAD-502

Plus, Konica Minolta, Japan) in the middle third of the leaf in the longitudinal direction. The complete above-ground part of the plant was harvested, and fresh biomass was determined. The whole root system was gently shaken to remove large soil particles, leaving soil attached to the roots, hereafter defined as rhizosphere soil[71]. The observed significant differences were evaluated by the Student's t-test or one-way ANOVA. We then performed Principal Component Analysis (PCA), which was applied to reduce the dimension of the original variables using the prcomp package in R software (v.4.1.3), and used the hclust package for Hierarchical Clustering Analysis (HCA).

Each plant's rooting system was subsampled for assessment of multiple response variables: root metabolomics for flavonoids metabolite analysis, root transcriptome analysis, and rhizosphere soils for 16S rRNA amplicon-based sequencing. Only fine roots (< 2 mm in diameter) were utilized for these responses. For metabolomics and transcriptomics, roots were quickly rinsed in deionized water and frozen in liquid nitrogen immediately. For rhizosphere soil, the qualified roots were collected in a 50-ml centrifuge tube containing 30 ml of sterile Phosphate Buffer Saline (PBS) buffer (pH 7.0, per liter: 6.33 g $NaH_2PO_4 \cdot H_2O$, 16.5 g $Na_2HPO_4 \cdot 7H_2O$, and 200 µl Silwet L-77) and stored on ice for further processing by the laboratory. In each plant, bulk soil samples were collected from around the root system and frozen in liquid nitrogen immediately. Rhizosphere samples were extracted from the corresponding root segments. Centrifuge tubes with samples were shaken for 30 min at 50 rpm in a constant-temperature shaker incubaror, and the shaking step was repeated twice. Afterwards, rhizosphere samples were centrifuged for 10 min at 4,000 rpm at 4 °C. The supernatant was then removed, and sterile water was added to resuspend the soil. Finally, the samples were frozen in liquid nitrogen and stored at -80 °C. All samples were stored at -80 °C until processed.

Establishment of the co-expression network

To unveil the intricate genetic regulatory network of poplar mediating microbial composition, the R package cluster (v.2.1.4) with the *k*-means method was used to

analyze the co-expression/co-regulation of flavonoids in root samples of nine poplars. Rigorous Pearson's correlation analysis was performed to identify the DEGs and OTUs ($r \geq 0.7$, P-values < 0.01) that were significantly associated with each flavonoid using the WGCNA (v.1.71) package.

Correlation analysis of modules

Correlation analyses between modules were carried out as previously described by the Pearson correlation coefficient[72]. Correlation analysis of Mantel tests was performed using the vegan (v.2.6-2) package between modules and microbiological families. The networks were visualized using Cytoscape (v.3.9.1)[73].

Pseudomonads swarming motility assay

The swarming motility experiment followed previously described with minor modifications [40]. Briefly, *Pseudomonas* strains were cultured in liquid King's B (KB) medium for 12 h until reaching a turbidity of 1.0 at 600 nm. Tricin and apigenin were separately prepared as 1 mM and 10 mM stock solutions in DMSO. Flavones at final concentrations of 1, 3, 5, 10, 20, 30, 50, and 100 μM were added to semi-solid Luria-Bertani (LB) medium containing 0.3% (w/v) agar in proportion to the volume. DMSO was added in equal volume to the negative control and then used after condensation. Data were collected at 12 h after inoculation. Each experiment was performed using three independent agar plates.

Data availability

The raw amplicon data are publicly accessible in the Genome Sequence Archive of the Beijing Institute of Genomics BIG Data Center, Chinese Academy of Sciences, under CRA015093. The root transcriptome could be accessed under CRA015096.

Author contributions

DZ and JX designed the experiments. JW, SL and YW collected and analyzed the data. JW, SL and YW performed the experiments. JW and JX wrote the manuscript. JS, SC, ST and YD, ZJ, revised the manuscript. DZ and JX obtained funding and is responsible for this article. All authors read and approved the manuscript. JW and SL contributed equally to this work.

Acknowledgements

This work was supported by funding from the Fundamental Research Funds for the National Key R&D Program of China [2021YFD2201203, 2022YFD2201600, 2022YFD2200602]; the Project of the National Natural Science Foundation of China [32371906, 32022057, 31972954, 32170370]; Central Universities [QNTD202305]; Forestry and Grassland Science and Technology Innovation Youth Top Talent Project of China [2020132607].

Declaration of interests

The authors declare no competing interests.

References

1. Singh, G., Agrawal, H. & Bednarek, P. Specialized metabolites as versatile tools in shaping plant–microbe associations. *Mol. Plant.* **16**, 122-144 (2023).
2. Wang, L. et al. Multifaceted roles of flavonoids mediating plant-microbe interactions. *Microbiome*. **10**, 233 (2022).
3. Xie, J. et al. Multifeature analysis of age-related microbiome structures reveals defense mechanisms of *Populus tomentosa* trees. *New Phytol.* **238**, 1636-1650 (2023).
4. Zhong, Y. et al. Root-secreted bitter triterpene modulates the rhizosphere microbiota to improve plant fitness. *Nat. Plants*. **8**, 887-896 (2022).
5. Peck, M. C., Fisher, R. F. & Long, S. R. Diverse flavonoids stimulate NodD1 binding to nod gene promoters in *Sinorhizobium meliloti*. *J. Bacteriol.* **188**, 5417-5427 (2006).
6. Broughton, W. J., Jabbouri, S. & Perret, X. Keys to symbiotic harmony. *J. Bacteriol.* **182**, 5641-5652 (2000).
7. Stringlis, I. A. et al. MYB72-dependent coumarin exudation shapes root microbiome assembly to promote plant health. *Proc. Natl. Acad. Sci. U. S. A.* **115**, E5213-E5222 (2018).
8. Carter, J. P., Spink, J., Cannon, P. F., Daniels, M. J. & Osbourn, A. E. Isolation, characterization, and avenacin sensitivity of a diverse collection of cereal-root-colonizing fungi. *Appl. Environ. Microbiol.* **65**, 3364-3372 (1999).
9. Leveau, A. et al. Towards take-all control: a C-21β oxidase required for acylation of triterpene defence compounds in oat. *New Phytol.* **221**, 1544-1555 (2019).
10. Turner, T. R. et al. Comparative metatranscriptomics reveals kingdom level changes in the rhizosphere microbiome of plants. *Isme J.* **7**, 2248-2258 (2013).
11. Zhou, C. J. et al. Evaluation of genetic diversity and germ plasm identification of 44 species, clones, and cultivars from 5 sections of the genus *Populus* based on amplified fragment length polymorphism analysis. *Ptant Molecular Biology Reporter*. **23**, 39-51 (2005).

12. Veach, A. M. et al. Rhizosphere microbiomes diverge among *Populus trichocarpa* plant-host genotypes and chemotypes, but it depends on soil origin. *Microbiome*. **7**, 76 (2019).
13. Attia, Z., Domec, J., Oren, R., Way, D. A. & Moshelion, M. Growth and physiological responses of isohydric and anisohydric poplars to drought. *J. Exp. Bot.* **66**, 4373-4381 (2015).
14. Gan, H. et al. Phosphorus and nitrogen physiology of two contrasting poplar genotypes when exposed to phosphorus and/or nitrogen starvation. *Tree Physiol.* **36**, 22-38 (2015).
15. Luo, J. & Zhou, J. Growth performance, photosynthesis, and root characteristics are associated with nitrogen use efficiency in six poplar species. *Environ. Exp. Bot.* **164**, 40-51 (2019).
16. Kumar, S. et al. Rice breeding for yield under drought has selected for longer flag leaves and lower stomatal density. *J. Exp. Bot.* **72**, 4981-4992 (2021).
17. Conti, L. et al. Functional trait differences and trait plasticity mediate biotic resistance to potential plant invaders. *J. Ecol.* **106**, 1607-1620 (2018).
18. Cregger, M. A. et al. The *Populus* holobiont: dissecting the effects of plant niches and genotype on the microbiome. *Microbiome*. **6**, 31 (2018).
19. Lin, T. et al. Drought stress-mediated differences in phyllosphere microbiome and associated pathogen resistance between male and female poplars. *The Plant Journal*. **115**, 1100-1113 (2023).
20. Guo, Q., Liu, L., Liu, J., Korpelainen, H. & Li, C. Plant sex affects plant-microbiome assemblies of dioecious *Populus cathayana* trees under different soil nitrogen conditions. *Microbiome*. **10**, 191 (2022).
21. Yan, D. et al. Genetic modification of flavone biosynthesis in rice enhances biofilm formation of soil diazotrophic bacteria and biological nitrogen fixation. *Plant Biotechnol. J.* **20**, 2135-2148 (2022).
22. Zhang, J. et al. NRT1.1B is associated with root microbiota composition and nitrogen use in field-grown rice. *Nat. Biotechnol.* **37**, 676-684 (2019).
23. Moreau, D., Bardgett, R. D., Finlay, R. D., Jones, D. L., and Philippot, L. A plant

perspective on nitrogen cycling in the rhizosphere. *Funct. Ecol*. **33**, 540-552 (2019).
24. Li, P. et al. Combined metagenomic and metabolomic analyses reveal that *Bt* rice planting alters soil C-N metabolism. *Isme J.* **3**, 4 (2023).
25. Song, Y. et al. FERONIA restricts *Pseudomonas* in the rhizosphere microbiome via regulation of reactive oxygen species. *Nat. Plants*. **7**, 644-654 (2021).
26. Escudero-Martinez, C. et al. Identifying plant genes shaping microbiota composition in the barley rhizosphere. *Nat. Commun.* **13**, 3443 (2022).
27. Zhong, C. et al. Multi-omics profiling reveals comprehensive microbe-plant-metabolite regulation patterns for medicinal plant *Glycyrrhiza uralensis* Fisch. *Plant Biotechnol. J.* **20**, 1874-1887 (2022).
28. Wallace, J. G., Kremling, K. A., Kovar, L. L. & Buckler, E. S. Quantitative Genetics of the Maize Leaf Microbiome. *Phytobiomes Journal*. **2**, 208-224 (2018).
29. Deng, S. et al. Genome wide association study reveals plant loci controlling heritability of the rhizosphere microbiome. *Isme J.* **15**, 3181-3194 (2021).
30. Li, Z. et al. Genotype-Specific Recruitment of Rhizosphere Bacteria From Sandy Loam Soil for Growth Promotion of *Cucumis sativus var. hardwickii*. *Front. Microbiol.* **13**, (2022).
31. Schmitz, L. et al. Synthetic bacterial community derived from a desert rhizosphere confers salt stress resilience to tomato in the presence of a soil microbiome. *Isme J*. **16**, 1907-1920 (2022).
32. Sibponkrung, S. et al. Co-Inoculation of *Bacillus velezensis* Strain S141 and *Bradyrhizobium* Strains Promotes Nodule Growth and Nitrogen Fixation. *Microorganisms (Basel)*. **8**, 678 (2020).
33. Pérez Rodriguez, M. M. et al. Halotolerant native bacteria *Enterobacter* 64S1 and *Pseudomonas* 42P4 alleviate saline stress in tomato plants. *Physiol. Plant.* **174**, (2022).
34. Wu, X. et al. Insight to key diazotrophic community during composting of dairy manure with biochar and its role in nitrogen transformation. *Waste Manage.* **105**, 190-197 (2020).
35. Guo, M. et al. Microbial mechanisms controlling the rhizosphere effect of ryegrass

on degradation of polycyclic aromatic hydrocarbons in an aged-contaminated agricultural soil. *Soil Biology and Biochemistry*. **113**, 130-142 (2017).

36. Yu, P. et al. Plant flavones enrich rhizosphere Oxalobacteraceae to improve maize performance under nitrogen deprivation. *Nat. Plants*. **7**, 481-499 (2021).
37. He, D. et al. Flavonoid-attracted *Aeromonas* sp. from the Arabidopsis root microbiome enhances plant dehydration resistance. *Isme J*. **16**, 2633 (2022).
38. Lam, P. Y., Liu, H. & Lo, C. Completion of Tricin Biosynthesis Pathway in Rice: Cytochrome P450 75B4 Is a Unique Chrysoeriol 5′-Hydroxylase. *Plant Physiol.* **168**, 1527-1536 (2015).
39. Shih, C. H. et al. Functional characterization of key structural genes in rice flavonoid biosynthesis. *Planta*. **228**, 1043-1054 (2008).
40. Yu, X. Q., Yan, X., Zhang, M. Y., Zhang, L. Q. & He, Y. X. Flavonoids repress the production of antifungal 2,4-DAPG but potentially facilitate root colonization of the rhizobacterium *Pseudomonas fluorescens*. *Environ. Microbiol.* **22**, 5073-5089 (2020).
41. Maximiano, M. R. et al. Proteome responses of *Rhizobium tropici* CIAT 899 upon apigenin and salt stress induction. *Appl. Soil Ecol.* **159**, 103815 (2021).
42. Stracke, R. et al. Differential regulation of closely related R2R3-MYB transcription factors controls flavonol accumulation in different parts of the *Arabidopsis thaliana* seedling. *Plant. J.* **50**, 660-677 (2007).
43. Wang, L. et al. AMYB/bHLH complex regulates tissue-specific anthocyanin biosynthesis in the inner pericarp of red-centered kiwifruit *Actinidia chinensis* cv. Hongyang. *The Plant Journal*. **99**, 359-378 (2019).
44. Peng, Y. & Zhu, G. Biological nitrogen removal with nitrification and denitrification via nitrite pathway. *Appl. Microbiol. Biotechnol.* **73**, 15-26 (2006).
45. Yang, R. et al. The natural pyrazolotriazine pseudoiodinine from *Pseudomonas mosselii* 923 inhibits plant bacterial and fungal pathogens. *Nat. Commun.* **14**, 734 (2023).
46. Martínez-Granero, F. et al. The Gac-Rsm and SadB signal transduction pathways converge on AlgU to downregulate motility in *Pseudomonas fluorescens*. *Plos One*.

659 **7**, e31765 (2012).
660 47. Catherine Bellini, D. I. P. and Perrone, A. I. Adventitious Roots and Lateral Roots:
661 Similarities and Adventitious Roots and Lateral Roots: Similarities and Differences.
662 *Plant Biol*. **65**, 639-66 (2014).
663 48. Ge, Y., Fang, X., Liu, W., Sheng, L. & Xu, L. Adventitious lateral rooting: the
664 plasticity of root system architecture. *Physiol. Plant.* **165**, 39-43 (2019).
665 49. Sheng, L. et al. Non-canonical *WOX11*-mediated root branching contributes to
666 plasticity in Arabidopsis root system architecture. *Development.***144**, 3126-3133
667 (2017).
668 50. Motte, H., Vanneste, S. & Beeckman, T. Molecular and Environmental Regulation
669 of Root Development. *Annu. Rev. Plant Biol.* **70**, 465-488 (2019).
670 51. Li, Q. et al. Plant growth-promoting rhizobacterium *Pseudomonas* sp. CM11
671 specifically induces lateral roots. *New Phytol.* **235**, 1575-1588 (2022).
672 52. Qi, T. et al. The Jasmonate-ZIM-Domain Proteins Interact with the WD-
673 Repeat/bHLH/MYB Complexes to Regulate Jasmonate-Mediated Anthocyanin
674 Accumulation and Trichome Initiation in *Arabidopsis thaliana*. *The Plant Cell*. **23**,
675 1795-1814 (2011).
676 53. Lan, J. et al. TCP transcription factors suppress cotyledon trichomes by impeding
677 a cell differentiation-regulating complex. *Plant Physiol.* **186**, 434-451 (2021).
678 54. Li, Y. et al. Volatile compounds from beneficial rhizobacteria *Bacillus* spp.
679 promote periodic lateral root development in Arabidopsis. *Plant, Cell &*
680 *Environment*. **44**, 1663-1678 (2021).
681 55. Yang, K. M. et al. RIN enhances plant disease resistance via root exudate-mediated
682 assembly of disease-suppressive rhizosphere microbiota. *Mol. Plant.* **16**, 1379-
683 1395 (2023).
684 56. Liu, H., Brettell, L. E., Qiu, Z. & Singh, B. K. Microbiome-Mediated Stress
685 Resistance in Plants. *Trends Plant Sci.* **25**, 733-743 (2020).
686 57. Liu, H. et al. Evidence for the plant recruitment of beneficial microbes to suppress
687 soil-borne pathogens. *New Phytol.* **229**, 2873-2885 (2021).
688 58. Korenblum, E., Massalha, H. & Aharoni, A. Plant-microbe interactions in the

689 rhizosphere via a circular metabolic economy. *The Plant Cell*. **34**, 3168-3182
690 (2022).
691 59. Brachi, B. et al. Plant genetic effects on microbial hubs impact host fitness in
692 repeated field trials. *Proceedings of the National Academy of Sciences*. **119**,
693 e2201285119 (2022).
694 60. Zhang, L. et al. A highly conserved core bacterial microbiota with nitrogen-fixation
695 capacity inhabits the xylem sap in maize plants. *Nat. Commun.* **13**, 3361 (2022).
696 61. Ashley Shade, A. N. S. Abundance-occupancy distributions to prioritize plant core
697 microbiome membership. *Curr. Opin. Microbiol.*, (2019).
698 62. Chen, X. et al. Nicotiana tabacum seed endophytic communities share a common
699 core structure and genotype-specific signatures in diverging cultivars. *Comp. Struct.*
700 *Biotechnol. J.* **18**, 287-295 (2020).
701 63. Zheng, Y. et al. Core root-associated prokaryotic community and its relationship
702 to host traits across wheat varieties. *J. Exp. Bot.* **74**, 2740-2753 (2023).
703 64. Liu, L. et al. Transgenic soybean of *GsMYB10* shapes rhizosphere microbes to
704 promote resistance to aluminum (Al) toxicity. *J. Hazard. Mater.* **455**, 131621
705 (2023).
706 65. Rüger, L. et al. Root cap is an important determinant of rhizosphere microbiome
707 assembly. *New Phytologist*. **239**, 1434-1448 (2023).
708 66. Liu, Q., Cheng, L., Nian, H., Jin, J. & Lian, T. Linking plant functional genes to
709 rhizosphere microbes: a review. *Plant Biotechnol. J.* **21**, 902-917 (2023).
710 67. Ditengou, F. A., Beguiristain, T. & Lapeyrie, F. Root hair elongation is inhibited
711 by hypaphorine, the indole alkaloid from the ectomycorrhizal fungus *Pisolithus*
712 *tinctorius*, and restored by indole-3-acetic acid. *Planta*. **211**, 722-728 (2000).
713 68. Woll, K. et al. Isolation, Characterization, and Pericycle-Specific Transcriptome
714 Analyses of the Novel Maize Lateral and Seminal Root Initiation Mutant *rum1*.
715 *Plant Physiol.* **139**, 1255-1267 (2005).
716 69. Felten, J. et al. The Ectomycorrhizal Fungus *Laccaria bicolor* Stimulates Lateral
717 Root Formation in Poplar and Arabidopsis through Auxin Transport and Signaling.
718 *Plant Physiol.* **151**, 1991-2005 (2009).

70. Schneider, C. A., Rasband, W. S. & Eliceiri, K. W. NIH Image to ImageJ: 25 years of image analysis. *Nat. Methods*. **9**, 671-675 (2012).
71. Edwards, J. et al. Structure, variation, and assembly of the root-associated microbiomes of rice. *Proceedings of the National Academy of Sciences*. **112**, (2015).
72. Bartoschek, M. et al. Spatially and functionally distinct subclasses of breast cancer-associated fibroblasts revealed by single cell RNA sequencing. *Nat. Commun.* **9**, (2018).
73. Shannon, P. et al. Cytoscape: a software environment for integrated models of biomolecular interaction networks. *Genome Res.* **13**, 2498-2504 (2003).

Figures

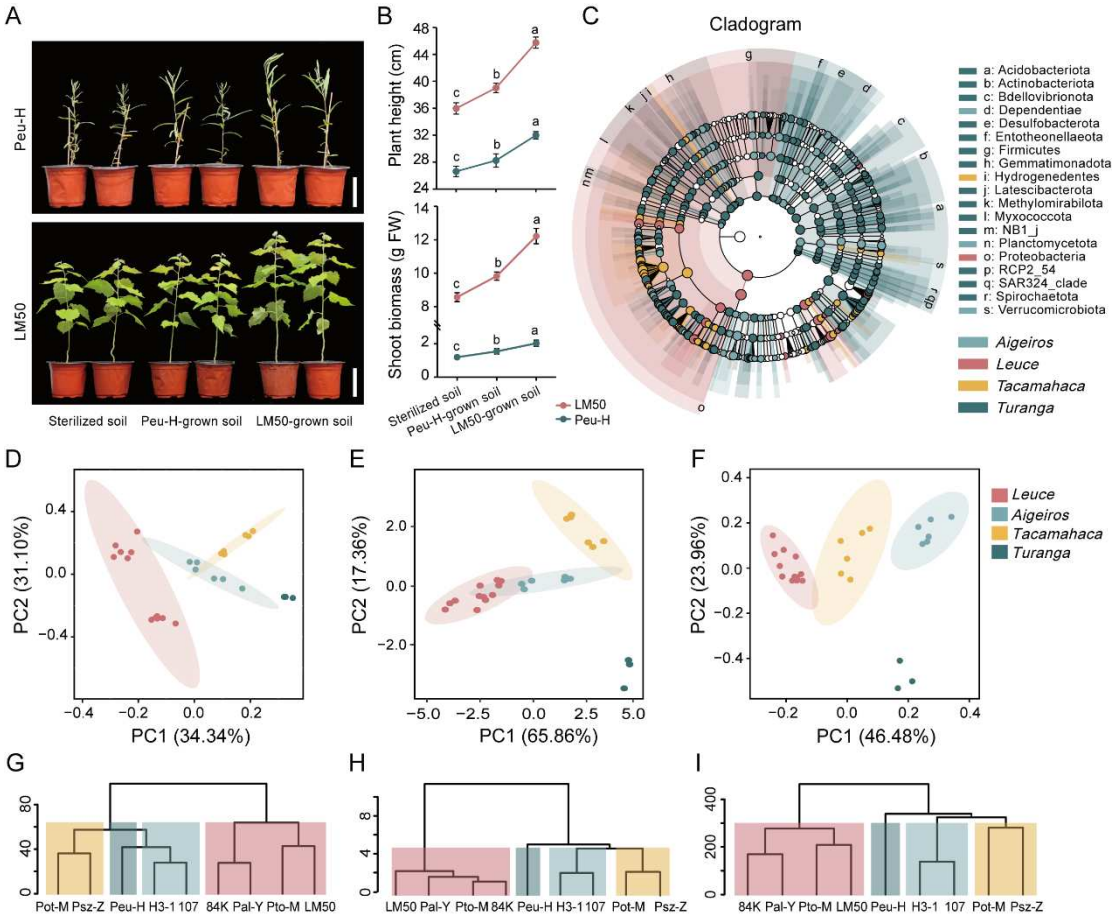

Fig. 1 The specific microbial taxa recruited by the poplar rhizosphere may be associated with plant performance. (A) Morphological differences of LM50 and Peu-H transplants in different soils (LM50-grown soil or Peu-H-grown soil). **(B)** Plant height and fresh shoot biomass of LM50 and Peu-H transplants in different soils (LM50-grown soil or Peu-H-grown soil). $n = 3$ biologically independent samples. **(C)** Linear discriminant analysis effect size (LEfSe) was performed to identify the rhizosphere bacteria that are differentially represented between the different poplar sections. From the inside to the outside, the sequence is boundary - phylum - class - order - family - genus. Each node represents a species, and the larger the node, the higher the abundance. The letters represent different phyla, and the colors indicate that the species is significantly different in the corresponding section (LDA score > 2, Kruskal-Wallis test, FDR adjusted *P*-values < 0.05). Principal Component Analysis

(PCA) and Hierarchical Clustering Analysis (HCA) of the microbiome **(D**, **G;** OTU > 2**)**, phenotype **(E**, **H)**, and transcriptome (**F**, **I**; TPM > 0) datasets from the nine poplar species. Different letters indicate significantly different groups (One-way ANOVA, *P*-values < 0.05). FW, fresh weight. Scale bars: (A) 10 cm.

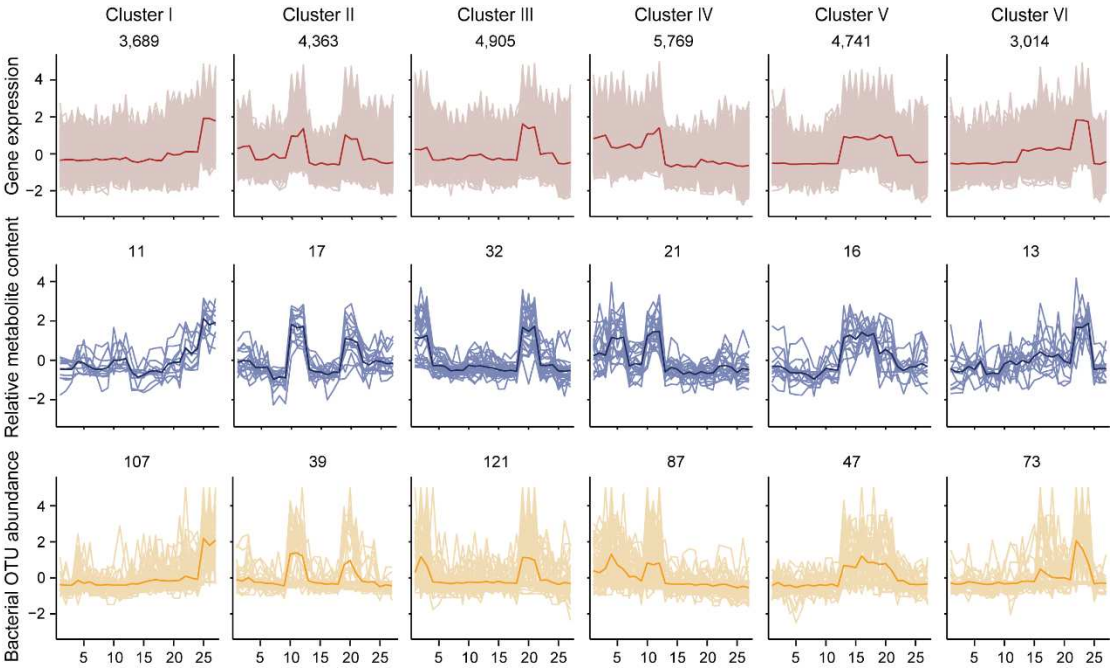

Fig. 2 Co-expression network of the transcriptome, metabolome, and microbiome. The *k*-means clustering algorithm and Pearson's correlation analysis ($r \geq 0.7$, *P*-values < 0.01) divided poplar gene expression profiles (red), flavonoid metabolome expression profiles (blue), and microbiome (OTUs; orange) into six clusters. The X-axis depicts 27 samples from nine poplar species, and the Y-axis depicts the Z-scores standardized for each gene, flavonoid, and OTU. The numbers shown in each box (for example, 3,689 genes, 11 flavonoids, and 107 OTUs for Cluster I) come from the number of genes, flavonoids, and OTUs for all 27 samples in each cluster. The numbers on the X-axis represent the samples: 1-3, Pto-M; 4-6, 84K; 7-9, Pal-Y; 10-12, LM50; 13-15, H3-1; 16-18, 107; 19-21, Pot-M; 22-24, Psz-Z; 25-27, Peu-H. The genes of Cluster I were enriched in *Turanga* (higher expression than at least one section; $|\log2FC| > 1$, *P*-values < 0.05) and the genes of Cluster IV were enriched in *Leuce* (higher expression than at least one section; $|\log2FC| > 1$, *P*-values < 0.05).

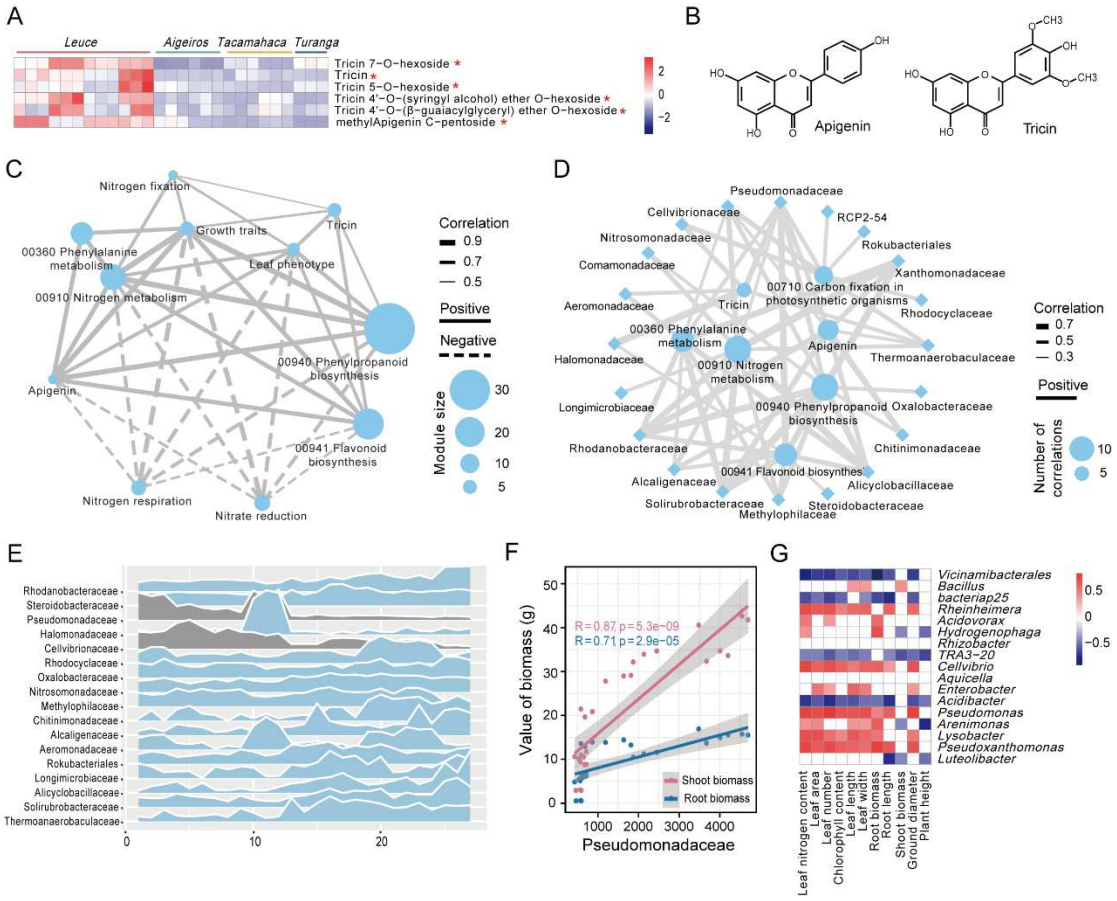

Fig. 3 Gene expression and flavonoid accumulation were related to rhizosphere microbial composition and poplar growth performance. (A) Apigenin and tricin (including derivatives) heat map in the root systems of different poplar sections. 27 samples correspond to different colors (each color corresponds to one section). Asterisks denote the flavones that were enriched in *Leuce* (One-way ANOVA, *P*-values < 0.05). **(B)** Chemical structure formulas for apigenin and tricin. **(C)** Correlation network of nitrogen cycle microbe modules, flavone modules, gene modules, and growth trait modules (*P*-values < 0.01). The microbe modules (nitrogen fixation, nitrate reduction, and nitrogen respiration) are functional modules of the FAPROTAX annotation in Cluster I or Cluster IV. The gene modules (00910 nitrogen metabolism, 00360 phenylalanine metabolism, 00940 phenylpropanoid biosynthesis, and 00941 flavonoid biosynthesis) are modules of KEGG enrichment analysis in Cluster IV. The flavone modules are apigenin (with derivatives) and tricin (with derivatives) of Cluster IV. Growth traits (including plant height, ground diameter, shoot biomass, root biomass,

and root length) and leaf traits (including leaf length, leaf width, leaf area, and leaf number). The node size represents the number of elements included (for example, the Growth traits module has 5 traits). Solid and dashed edges indicate positive and negative relationships, respectively. Edge thickness denotes the strength of correlations. **(D)** Correlation network of the top 50 microbial families with flavone modules and gene modules of Cluster IV (*P*-values < 0.01). Solid edges indicate positive relationships. Edge thickness denotes the strength of correlations. **(E)** Relative abundance profles of dominant families. The numbers on the X-axis represent the samples: 1-3, Pto-M; 4-6, 84K; 7-9, Pal-Y; 10-12, LM50; 13-15, H3-1; 16-18, 107; 19-21, Pot-M; 22-24, Psz-Z; 25-27, Peu-H. **(F)** Pearson's correlation between Pseudomonadaceae and the shoot and root biomass of poplars. **(G)** Pearson's correlation between dominant genera and 11 characteristics of poplars. The color of the heat map represents the size of the correlation coefficient.

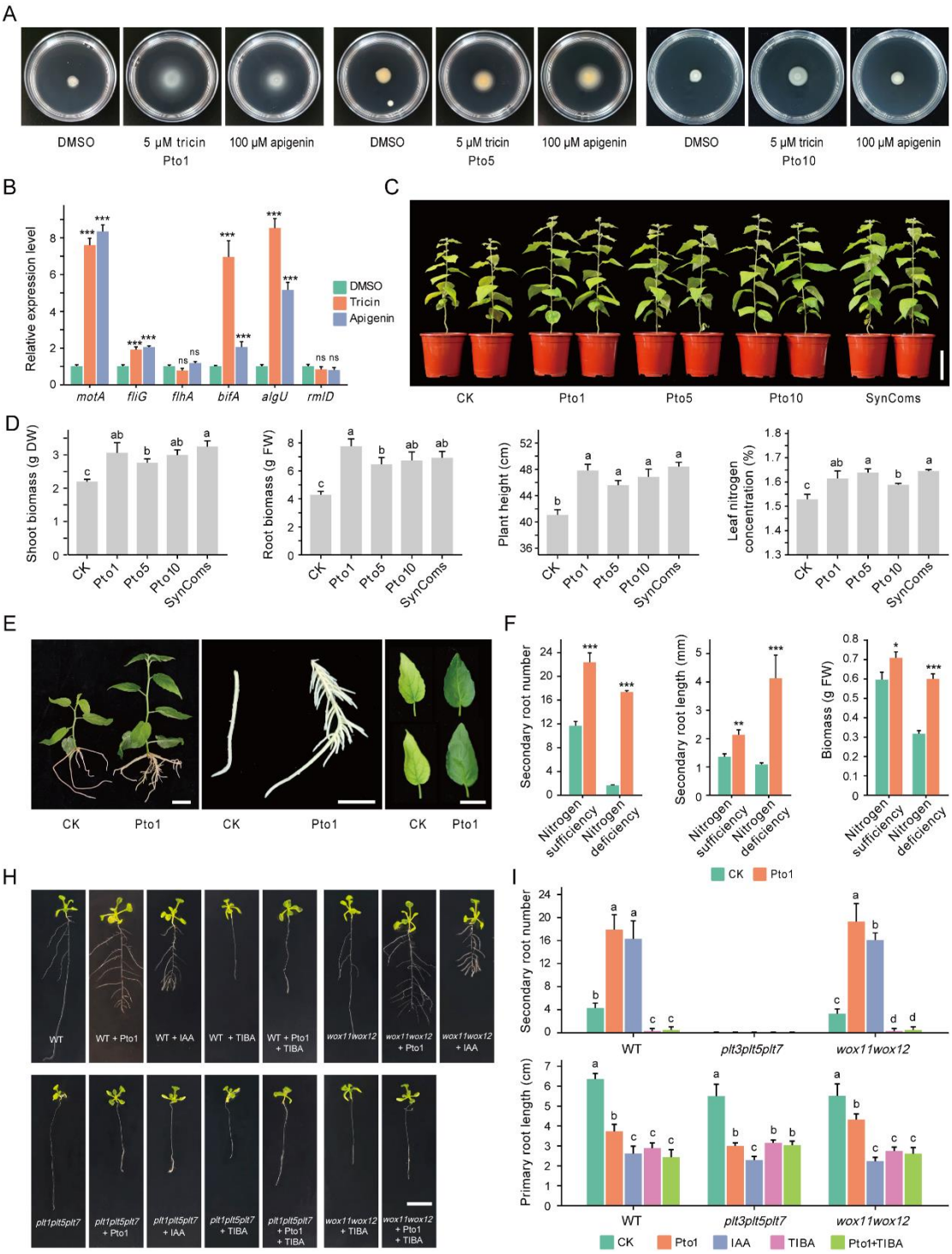

Fig. 4 Flavone-mediated pseudomonads promote nitrogen uptake and lateral root growth in poplar. (A) Swarming motility of *Pseudomonas* strains Pto1, Pto5, and Pto10 on 0.3% agar medium in the presence of either 5 μM tricin or 100 μM apigenin. **(B)** qRT-PCR assays revealed that flagellar-related genes (*motA*, *fliG*, *flhA*, and *bifA*) and biofilm formation-related genes (*algU* and *rmlD*) expression were induced by tricin

and apigenin. **(C)** Pot experiment of inoculating poplar with pseudomonads in nitrogen-poor soil. **(D)** Dry shoot biomass, fresh root biomass, plant height, and leaf nitrogen concentration of poplar inoculated with pseudomonads in nitrogen-poor soil. $n = 3$ biologically independent samples. **(E)** Growth differences of poplars inoculated with Pto1 in sterile nitrogen-poor culture medium. Whole plant (left), root (middle), leaf (right). **(F)** The secondary root number, secondary root length, and total fresh biomass of poplars inoculated with Pto1 in sterile nitrogen-poor medium and sterile nitrogen-rich medium. $n = 3$ biologically independent samples. **(H)** Growth differences of wild-type (WT), *plt3plt5plt7*, and *wox11wox12* Arabidopsis seedlings growing on 1/2 MS agar plates with Pto1, IAA, TIBA, Pto1 + TIBA, or mock. **(I)** Quantification of secondary root (SR) number and primary root length in WT, *plt3plt5plt7*, and *wox11wox12* Arabidopsis seedlings under mock, IAA, TIBA, Pto1 + TIBA, and Pto1 inoculated conditions. $n = 5$ biologically independent samples. Asterisks indicate significant differences between different groups (Student's t-test, ***P-values < 0.001, **P-values < 0.01, *P-values < 0.05, ns: not significant). Different letters indicate significantly different groups (One-way ANOVA, P-values < 0.05). DW, dry weight; FW, fresh weight. Scale bars: (C) 10 cm; (E) 1 cm; (H) 1 cm.

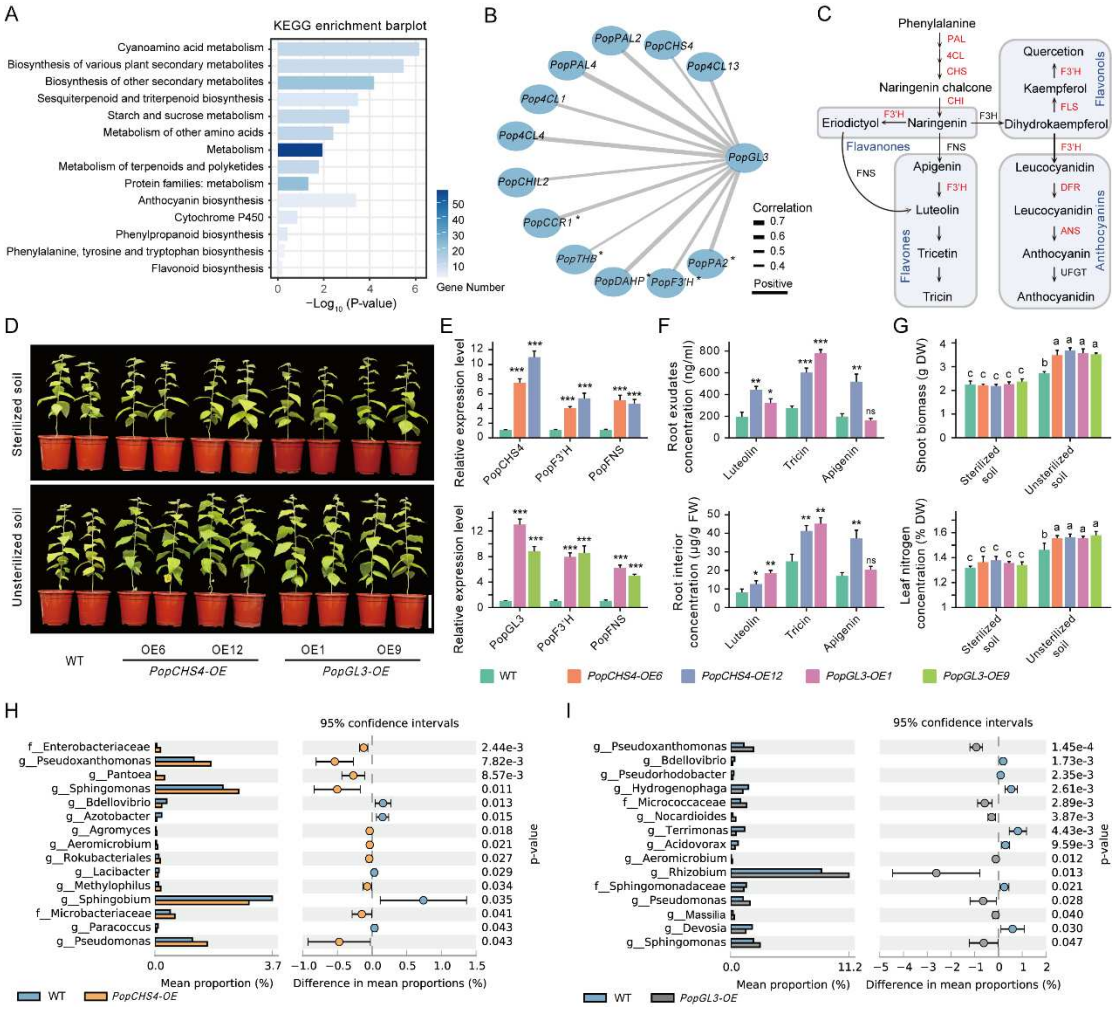

Fig. 5 *PopGL3* regulates tricin synthesis to recruit *Pseudomonas*. **(A)** KEGG enrichment analyses of DAP experimental analysis results for *PopGL3*. **(B)** A flavonoid-related gene network was established based on the DAP assay results of *PopGL3*. Pearson correlation coefficient values were calculated for each pair of genes. Solid edges indicate positive relationships. Edge thickness denotes the strength of correlations. Asterisks denote the genes that were the result of two repeats of the DAP experiment, and the other genes were the result of one repeat. **(C)** Schematic representation of flavonoid biosynthesis and regulation in poplar. The red font indicates genes regulated by *PopGL3* based on the DAP assay (results of at least one repeat). **(D)** Growth differences between WT, *PopCHS4-OE*, and *PopGL3-OE* poplar lines in sterilized or unsterilized nitrogen-poor soil. Gene relative expression level **(E)**, root interior and root exudate flavone concentration **(F)** of WT, *PopCHS4-OE*, and *PopGL3-*

OE poplar lines in unsterilized nitrogen-poor soil. $n = 3$ biologically independent samples. **(G)** Dry shoot biomass and leaf nitrogen concentration of WT, *PopCHS4-OE*, and *PopGL3-OE* poplar lines in sterilized or unsterilized nitrogen-poor soil. $n = 3$ biologically independent samples. Abundance differences between *PopCHS4-OE* **(H)** and *PopGL3-OE* **(I)** poplar lines and WT rhizosphere microbiomes at the genus level (two-sided Welch's t-test), some genera are unnamed and named after families. Asterisks indicate significant differences between different groups (Student's t-test, ****P*-values < 0.001, ***P*-values < 0.01, **P*-values < 0.05, ns: not significant). Different letters indicate significantly different groups (One-way ANOVA, *P*-values < 0.05). DW, dry weight; FW, fresh weight. Scale bar: (D) 15 cm.

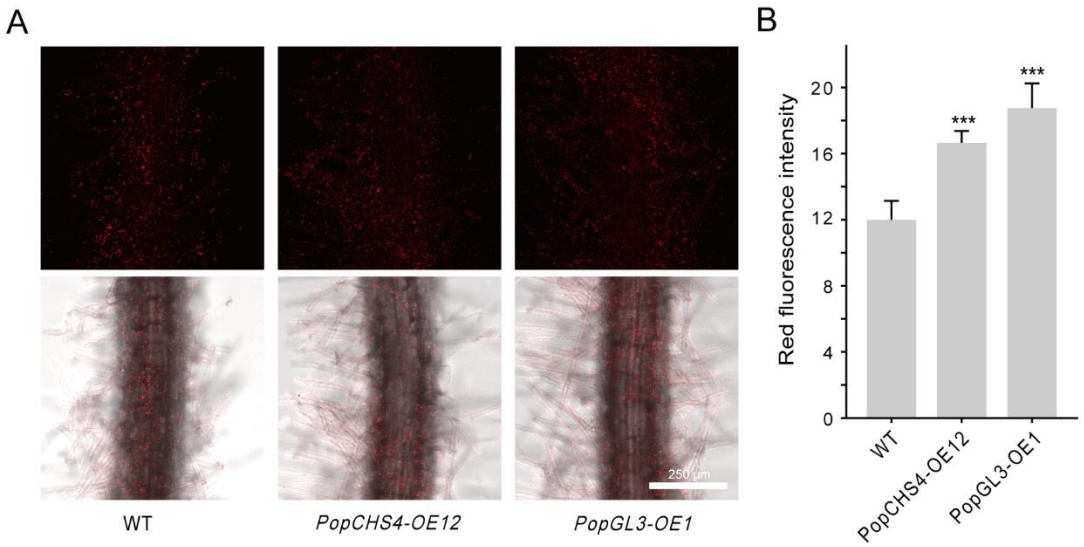

Fig. 6 *PopGL3* recruits pseudomonads to colonize poplar roots. (A) Confocal fluorescence imaging of RFP-tagged Pto1 colonizing poplar roots of different genotypes. **(B)** The fluorescence intensity of RFP in poplar roots of different genotypes. The fluorescence intensity of the samples was measured by confocal fluorescence microscopy. Asterisks indicate significant differences between different groups (Student's t-test, ****P*-values < 0.001). Scale bar: (A) 250 μm.

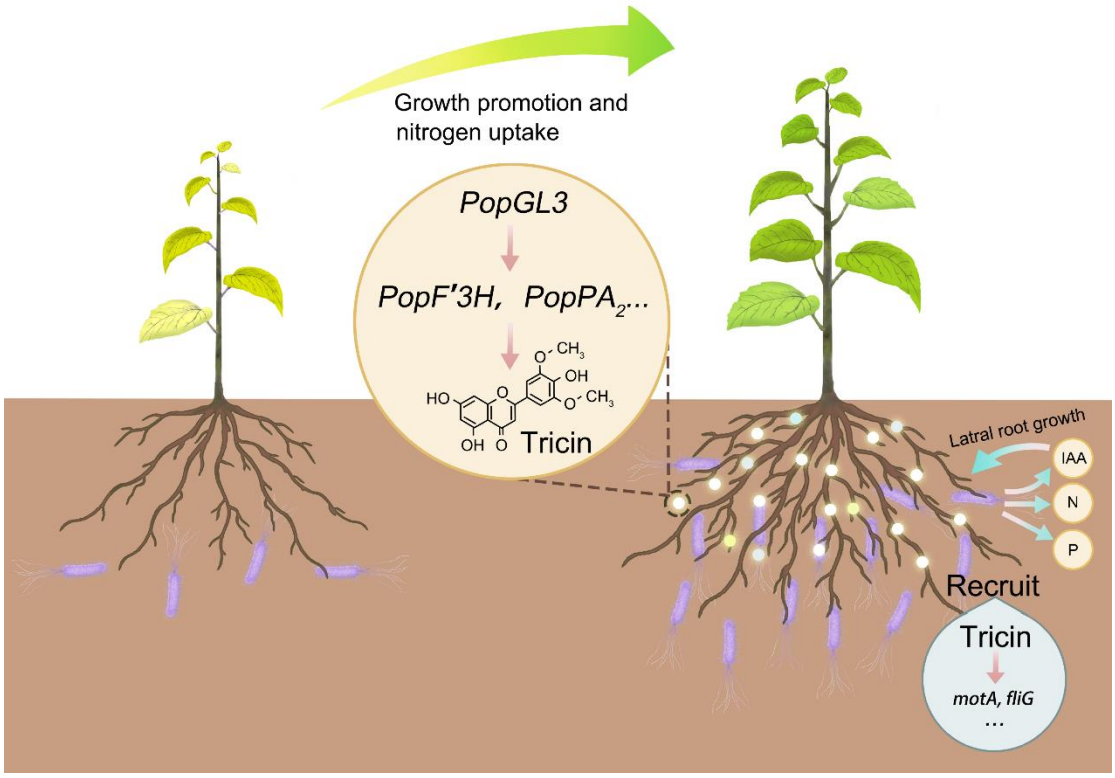

Fig. 7 Proposed model for flavone-dependent, microbiota-mediated lateral root formation and plant performance. In nitrogen-poor soil, poplar roots secreted flavone and recruited *Pseudomonas* to colonize the rhizosphere, thus changing the composition of the rhizosphere microbial community. By secreting auxin IAA, *Pseudomonas* can induce lateral root formation to promote plant growth and nitrogen absorption indirectly, and promote plant growth and nitrogen absorption directly through biological nitrogen fixation.

Supplementary Files

This is a list of supplementary files associated with this preprint. Click to download.

- Wuet.al.SupportingInformation20240313.pdf
- SupplementaryData.xls